MOLECULAR AND CELLULAR BIOLOGY, Jan. 1987, p. 512–522
0270-7306/87/010512-11$02.00/0

Vol. 7, No. 1

Identification of a New Common Provirus Integration Site in Gross Passage A Murine Leukemia Virus-Induced Mouse Thymoma DNA

RICHARD VILLEMUR,[1] YURY MONCZAK,[1] ERIC RASSART,[1,2] CHRISTINE KOZAK,[3] AND PAUL JOLICOEUR[1,4]*

Institut de Recherches Cliniques de Montréal, Montreal, Quebec, Canada H2W 1R7[1]; Département de Microbiologie et d'Immunologie[4] and Département de Médecine,[2] Université de Montréal, Montreal, Quebec, Canada H3C 3J7; and Laboratory of Molecular Microbiology, National Institute of Allergy and Infectious Diseases, Bethesda, Maryland 20892[3]

Received 7 July 1986/Accepted 6 October 1986

The Gross passage A murine leukemia virus (MuLV) induced T-cell leukemia of clonal (or oligoclonal) origin in inoculated mice. To study the role of the integrated proviruses in these tumor cells, we cloned several newly integrated proviruses (with their flanking cellular sequences) from a single tumor in procaryotic vectors. With each of the five clones obtained, a probe was prepared from the cellular sequences flanking the provirus. With one such probe (SS8), we screened several Gross passage A MuLV-induced SIM.S mouse tumor DNAs and found that, in 11 of 40 tumors, a provirus was integrated into a common region designated *Gin-1*. A 26-kilobase-pair sequence of *Gin-1* was cloned from two λ libraries, and a restriction map was derived. All proviruses were integrated as a cluster in the same orientation within a 5-kilobase-pair region of *Gin-1*, and most of them had a recombinant structure of the mink cell focus-forming virus type. The frequency of *Gin-1* occupancy by provirus was much lower in thymoma induced by other strains of MuLV in other mouse strains. Using somatic-cell hybrid DNAs, we mapped *Gin-1* on mouse chromosome 19. *Gin-1* was not homologous to 16 known oncogenes and was distinct from the other common regions for provirus integration previously described. Therefore, *Gin-1* appears to represent a new common provirus integration region. The integration of a provirus within *Gin-1* might be an important event leading to T-cell transformation, and the *Gin-1* region might harbor sequences which are involved in tumor development.

The acute transforming defective retroviruses harbor a cell-derived oncogene on their genomes and induce neoplasms after a short latent period. The oncogenic viral sequences have been shown to be primarily responsible for the initiation and maintenance of the transformed state (for a review, see references 1 and 55). In contrast, the nondefective slow-transforming retroviruses, such as avian leukosis virus, mouse mammary tumor virus, and murine leukemia virus (MuLV), generally induce malignant diseases of monoclonal or oligoclonal origin after a long latent period. These viruses do not harbor a cell-derived oncogene, but, as observed with different strains of MuLVs, the 3′ ends of their genomes, and more specifically the U3 long terminal repeat (LTR), seem important for tumor induction (4, 9–11, 23, 30).

The molecular mechanism by which these nondefective retroviruses induce cell transformation appears to operate by the insertion of their provirus in the vicinity of a cellular oncogene or of a gene involved in growth control. In a high proportion of avian leukosis virus-induced tumors, proviruses have been found to be inserted close to c-*myc* (20, 33, 37) and to c-*erbB* (15), leading to an increased transcription of these oncogenes. Two regions, *int-1* (34, 35) and *int-2* (12, 38), in DNA of mouse mammary tumor virus-induced mouse mammary carcinoma and one region, *int-41* (17), in DNA of mouse mammary tumor virus-induced kidney adenocarcinoma have been reported to represent common regions for provirus integration, whose transcription was activated by these insertions. In MuLV-induced T-cell lymphoma, c-*myc* (7, 31, 43, 49) and a putative new tyrosine kinase oncogene, *tck* (58), have been shown to be activated by provirus insertion. Similarly, c-*myb* (45, 46) and c-*mos* (3) were shown to be activated, in some MuLV-induced myeloid and B-cell tumors, respectively, by the integration of LTR sequences in their vicinity. Recently, the interleukin-2 (6) and interleukin-3 (59) genes were also found to be activated by nearby integration of LTR sequences in gibbon T-lymphoid MLA 144 and in mouse WEH1-3B myelomonocytic leukemia cell lines, respectively. Six other apparently distinct regions, designated *Mlvi-1*, *Mlvi-2*, *Mlvi-3* (51–54), *Mis-1/pvt-1* (18, 29, 57), *Pim-1* (8), and *Fis-1* (47), have been reported to be the sites of common provirus integrations in mouse or rat T-cell or myelogenous leukemic DNA and might represent putative new oncogenes. Among these, provirus insertions have been shown to activate the transcription of *Pim-1* (8, 44). Except for *Pim-1*, which is occupied by provirus in about 60% of the tumors induced by a specific strain of MuLV, i.e., the Moloney strain, these regions have been shown to harbor proviruses at a low frequency in MuLV-induced tumors, suggesting that other undetected genetic events, possibly integrations in other regions, were occurring.

To test this hypothesis and to identify new common proviral integration regions which could contain putative new oncogenes, we searched for such a region in Gross passage A (Gross A) MuLV-induced T-cell lymphoma. Gross A MuLV is a leukemogenic, nondefective, ecotropic, fibrotropic, and thymotropic virus which was initially derived from a spontaneous AKR tumor and subsequently was passaged serially in mice (2, 11, 19). Gross A MuLV induced thymoma in various mouse strains after a latent period of 4 to 8 months postinoculation. Its primary leukemogenic viral determinant has been shown to lie within the enhancer sequences of the U3 LTR (9, 11). By cloning several virus-host junction fragments of one Gross A MuLV-induced thymoma, we derived probes with the flanking

* Corresponding author.

cellular sequences and used them to search for provirus integration within the homologous region in other thymomas. With one such probe, we identified a region of chromosomal DNA in which proviruses were integrated relatively frequently. This region was designated *Gin-1* (Gross A MuLV integration site), and we report its characterization.

MATERIALS AND METHODS

Mice and viruses. Mice were from our breeding colony. The inbred SIM.S mice were originally obtained from A. Axelrad (University of Toronto, Toronto, Ontario, Canada). The outbred NIH/Swiss mice were obtained from Small Animal Resources (National Institutes of Health, Bethesda, Md.). Both strains were Fv-$1^{n/n}$ and were susceptible to Gross A MuLV (56). Newborn (<48-h-old) mice were inoculated intraperitoneally with 0.15 ml of filtered (pore size, 0.45 μm; Millipore Corp., Bedford, Mass.) tissue culture medium containing 10^5 PFU of pGD-17 MuLV, a molecularly cloned derivative of Gross A MuLV (56). Leukemia developed 4 to 8 months postinoculation, and mice were sacrificed when they were moribund.

DNA extraction and endonuclease digestion. High-molecular-weight cellular DNA was prepared from primary thymomas or from livers by phenol extraction and was ethanol precipitated and digested with various restriction endonucleases (New England BioLabs, Inc., Beverly, Mass.; Boehringer Mannheim Biochemicals, Montreal; and P-L Pharmacia, Montreal) under the conditions recommended by the manufacturers as previously described (29). Bacteriophage and plasmid DNAs were prepared essentially as described elsewhere (32).

Agarose gel electrophoresis and hybridization procedure. DNA analysis by agarose gel electrophoresis and transfer to nitrocellulose membranes were done by the technique of Southern (48), as described previously (56). Specific DNA fragments were detected by hybridization with ^{32}P-labeled cloned DNA fragments. These cloned DNA fragments were excised from the vector with appropriate restriction endonucleases, and the inserts were separated from the vector by agarose gel electrophoresis. The DNA fragments were recovered by electroelution and ethanol precipitation, as described previously (9–11), and were used directly as hybridization probes. Probes were labeled by nick translation (41) or by incubating the denatured fragment in the presence of hexamers and the Klenow fragment of polymerase 1 (14). Filters were hybridized in 50% formamide, 3× SSC (1× SSC is 0.15 M NaCl plus 0.015 M sodium citrate), and Denhardt solution at 42°C. After hybridization, the filters were washed sequentially in 2× SSC for 15 min at room temperature, in 0.1× SSC–0.1% sodium dodecyl sulfate for 1 h at 55°C, and in 0.1× SSC for 2 min at room temperature. Membranes were air dried and exposed at −70°C to RP-Royal X-Omat film (Eastman Kodak Co., Rochester, N.Y.) with a Cronex Lightning-Plus intensifying screen (Du Pont Co., Wilmington, Del.).

Molecular cloning procedure. DNA from tumor 9 was digested with *Eco*RI and centrifuged on a sucrose density gradient (15 to 30%) as previously described (29). Fractions containing fragments from 10 to 20 and 2 to 10 kilobase pairs (kbp) were pooled separately and ethanol precipitated. DNA (0.5 μg) from each pool was then ligated respectively to *Eco*RI-cleaved Charon 4A arms (1 μg) or to *Eco*RI-cleaved λgtWES arms and was packaged as described elsewhere (29, 32). The MuLV recombinant phages (1.3 × 10^6 phages) were identified by hybridization with a mixture of ^{32}P-labeled ecotropic MuLV-specific AKV-5, AKV-6 (21), and eco (5) probes (Fig. 1), as previously described (32). Larger regions of *Gin-1* sequences were cloned by screening two libraries of lambda phages with a ^{32}P-labeled SS8 probe. One of the libraries was prepared in Charon 4A with partially digested *Eco*RI DNA from thymoma 9 (8 × 10^5 phages). The other library (kindly provided by J. G. Seidman, Harvard University, Cambridge, Mass.) was prepared in Charon 4A with partially digested *Hae*III DNA from a C57BL/6 mouse (10^6 phages). The 15- to 20-kbp partially digested thymoma 9 DNA fragments were enriched on sucrose density gradient and prepared for cloning as described above. Subcloning of

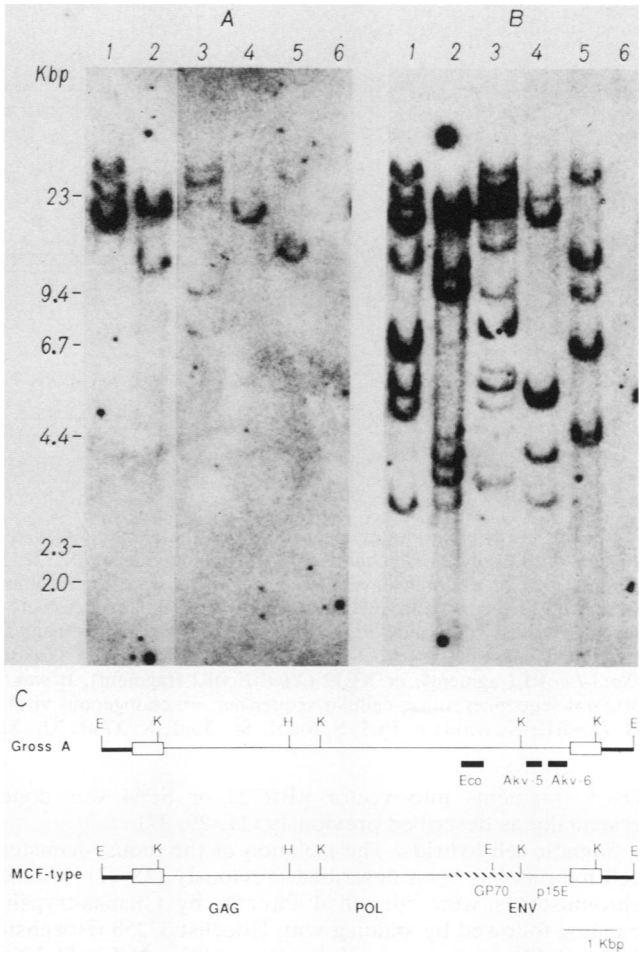

FIG. 1. Analysis of proviruses in Gross A MuLV-induced thymomas. DNAs from representative primary thymomas or from normal SIM.S mouse liver were digested with *Eco*RI, fractionated by electrophoresis on a 1% agarose gel, and transferred to nitrocellulose membrane as described in the text. The filter was then hybridized with ^{32}P-labeled ecotropic MuLV-specific probe eco (A) or AKV-5 (B). DNAs were from thymomas 6 (lane 1), 7 (lane 2), 8 (lane 3), 9 (lane 4), and 12 (lane 5) and from normal mouse liver (lane 6). (C) Partial restriction map of the viral genome from ecotropic Gross A MuLV and from an MCF-type MuLV (5, 21, 56). The localization of the sequences homologous to the eco, AKV-5, and AKV-6 probes is illustrated. The MCF-specific sequences extend in other regions in other classes of MCF MuLV (13). Fragment size was estimated with *Hin*dIII-digested λ DNA as markers. Symbols: ▭, LTR; ——, viral genome; ▬, cellular sequences; ∿∿, nonecotropic MCF-type recombinant sequences. Restriction sites: E, *Eco*RI; H, *Hin*dIII; K, *Kpn*I.

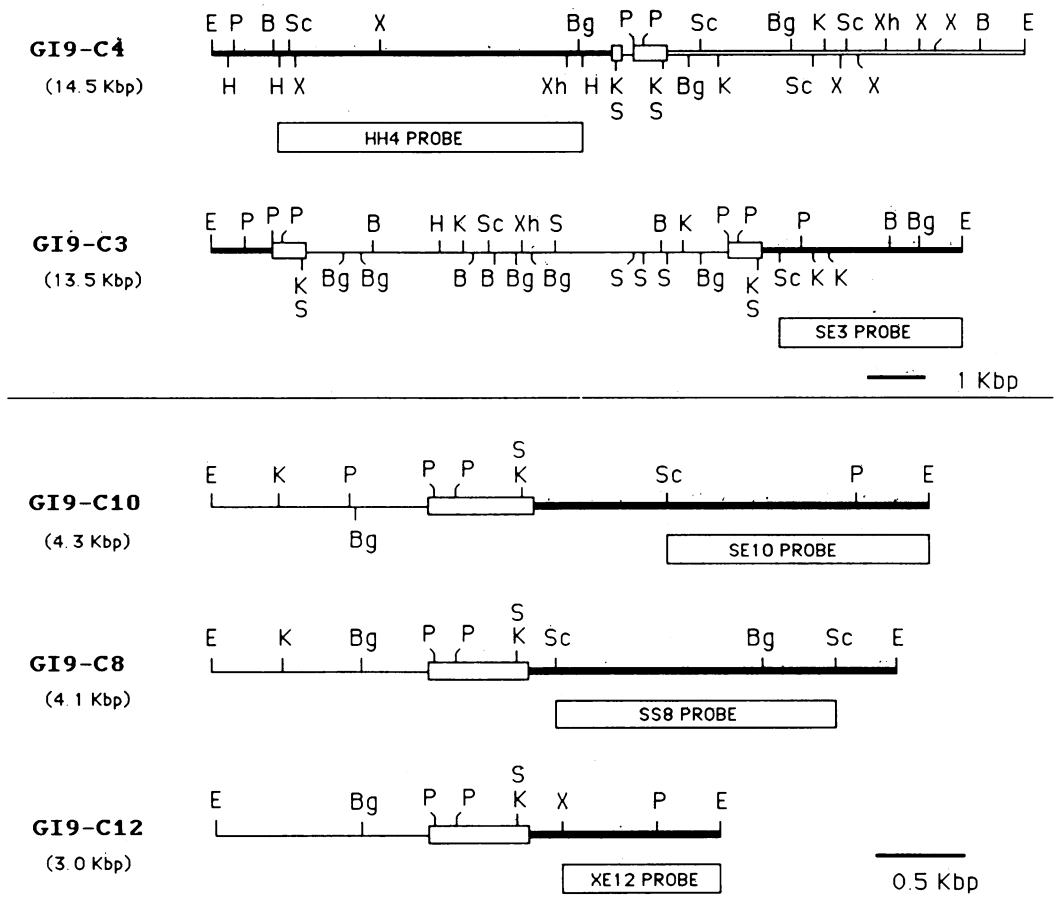

FIG. 2. Restriction endonuclease maps of the cloned Gross A MuLV proviruses from thymoma 9. The five recombinant phages were cleaved with *Eco*RI, and each insert was subcloned into pBR322. For mapping, each plasmid DNA was digested with *Eco*RI and then with other restriction endonucleases. DNA fragments were electrophoresed on a 1.4% agarose gel and visualized with ethidium bromide. They were transferred to nitrocellulose membranes and successively hybridized with ^{32}P-labeled eco, AKV-5, AKV-6, LTR-specific, and representative viral probes. Fragment size was estimated by using *Hin*dIII-digested λ DNA as markers. A cellular fragment of each clone was subcloned into an Sp64 vector and was designated HH4 (*Hin*dIII fragment), SE3 (*Sac*I-*Eco*RI fragment), SS8 (*Sac*I fragment), SE10 (*Sac*I-*Eco*RI fragment), or XE12 (*Xba*I-*Eco*RI fragment). It was then used as a single-copy hybridizing probe. Symbols: ——, Gross A proviral sequences; ▬, cellular sequences; ═, endogenous viral sequences; ▭, LTR. Restriction sites: B, *Bam*HI; Bg, *Bgl*I; E, *Eco*RI; H, *Hin*dIII; K, *Kpn*I; P, *Pst*I; S, *Sma*I; Sc, *Sac*I; X, *Xba*I; Xh, *Xho*I.

DNA fragments into vector pBR322 or SP64 was done essentially as described previously (11, 29, 32).

Somatic cell hybrids. The isolation of the mouse-hamster cell hybrids has been described previously (25–27). Mouse chromosomes were identified directly by Giemsa-trypsin banding followed by staining with Hoechst 33258 (Hoechst-Roussel Pharmaceuticals, Inc., Somerville, N.J.). Hybrid cells were typed for the presence of specific mouse markers as described previously (25–27).

RESULTS

Cloning of virus-cell junction fragments of thymoma 9. Gross A MuLV is a leukemogenic retrovirus able to induce a high percentage (80%) of T-cell leukemia (thymoma) in inoculated inbred SIM.S mice after a latent period of 4 to 8 months (2, 19, 56). To analyze the structure of the proviruses in the thymoma DNAs, we first performed a restriction endonuclease analysis by the Southern blot procedure (48). *Eco*RI was most suitable for this analysis because it did not cleave the ecotropic Gross A MuLV genome (56) and, therefore, with an *env* ecotropic MuLV-specific (eco) (5) probe, allowed the detection of each newly acquired ecotropic Gross A provirus flanked by cellular sequences (Fig. 1A). However, with another ecotropic MuLV-specific probe, AKV-5 (21), several additional newly integrated viral sequences, some of them smaller than the full-length genome (8.8 kbp), were detected in each tumor (Fig. 1B). The ecotropic MuLV-specific AKV-6 probe (Fig. 1) detected the same fragments as the AKV-5 probe (data not shown). These probes have previously been shown to detect mink cell focus-forming (MCF)-type recombinant proviruses (21). These MCF genomes harbor sequences from the ecotropic MuLV genome at the 3′ end of *env* and sequences from an endogenous nonecotropic genome at the 5′ end of *env* and the 3′ end of *pol* (21). They were also found to harbor an *Eco*RI site at position 6.9 (21). All 40 Gross A MuLV-induced thymomas screened appeared to harbor several recombinant proviruses of the MCF type; all of them also contained at least one provirus from the inoculated parental ecotropic Gross A MuLV. With the three probes used, each tumor DNA showed a specific and different set of virus-specific fragments, suggesting that these tumors were clonal (or oligoclonal) in origin.

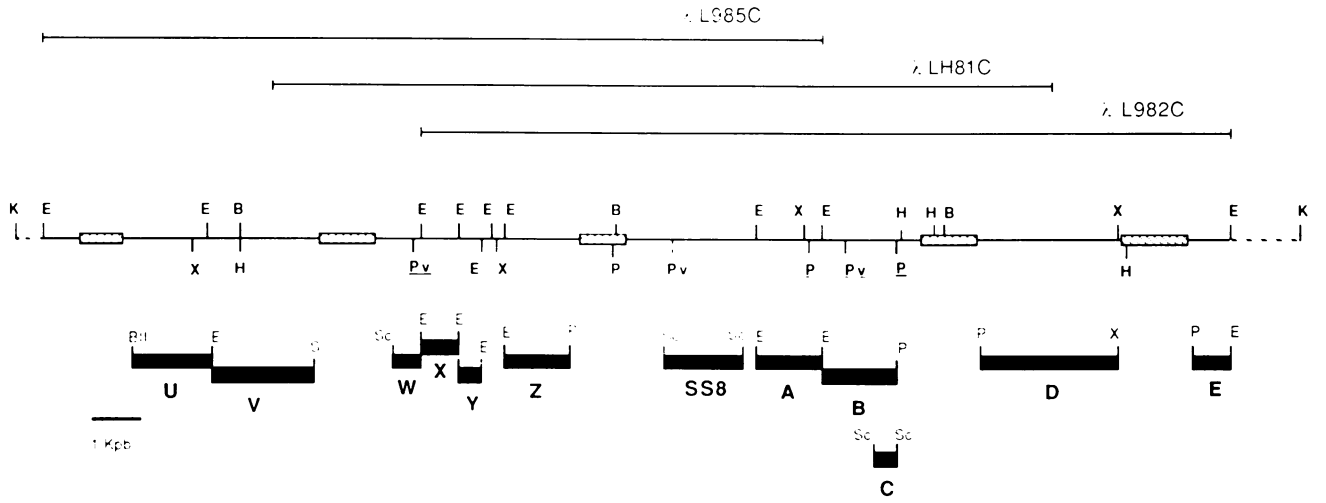

FIG. 3. Restriction endonuclease map of the *Gin-1* region. Three recombinant phages hybridizing with the SS8 probe were isolated from two mouse libraries and designated λ L985C, λ LH81C, and λ L982C. DNA from these clones was digested with various restriction endonucleases to derive a restriction map of the region, essentially as described in the legend to Fig. 2. The map was also confirmed by digesting normal mouse DNA with several restriction endonucleases alone and in combination, by using the SS8 probe. The *Kpn*I sites were mapped with a *Hin*dIII-*Kpn*I digestion of normal DNA hybridized with end probes U and E. Large fragments of the region were subcloned into pBR322, and smaller, nonreiterated fragments were isolated or subcloned into SP64 or pBR322, to be used as hybridizing probes (A to E and U to Z). Underlined restriction sites have not been mapped on the whole region. Symbols: ▨, highly reiterated sequences; ▬, fragments used as probes; – – –, uncloned sequences. Restriction sites: B, *Bam*HI, Bll, *Bgl*II; E, *Eco*RI; H, *Hin*dIII; K, *Kpn*I; P, *Pst*I; Pv, *Pvu*II; S, *Sma*I; Sc, *Sac*I; X, *Xba*I.

To study whether some of these proviruses were integrated in a common region of the cellular genome in different thymomas, we attempted to clone all the proviruses from a single tumor. We selected tumor 9, a tumor with a less complex pattern of viral insertions as revealed by hybridization with AKV-5 and AKV-6 probes (Fig. 1A and B, lanes 4). *Eco*RI-cleaved tumor 9 DNA was cloned in vectors Charon 4A and λgtWES by using eco, AKV-5, and AKV-6 as probes. Five of the six detectable proviruses were successfully cloned, subcloned into pBR322, and analyzed by restriction endonucleases and Southern blot analysis with eco, AKV-5, AKV-6, and representative and LTR-specific probes (data not shown). The restriction map of each of these clones is presented in Fig. 2. The GI9-C3 clone represents a full-length ecotropic Gross A provirus with its flanking cellular sequences. The GI9-C4 clone represents the 3′ end of Gross A p15E sequences and the Gross A LTR inserted within an endogenous mouse provirus. The GI9-C8, GI9-C10, and GI9-C12 clones represent the 3′ end of MCF-type recombinant Gross A proviruses flanked by cellular sequences. Indeed, these clones harbored the *Eco*RI site (at position 6.9), which is specific to MCF proviruses (13). All clones harbored the two *Pst*I sites within the LTR characteristic of the Gross A LTR (56). These results clearly showed that MCF-type recombinant MuLVs were present in Gross A MuLV-induced thymomas.

A cellular fragment from each clone was isolated, screened for the absence of repetitive sequence elements by hybridization to *Eco*RI-cleaved mouse DNA, and subcloned into SP64. These fragments were used as single-copy hybridization probes to search for common integration sites in other thymomas. A completed search with one probe (SS8) derived from clone GI9-C8 was positive, and we could detect rearrangement of this region in other thymoma DNAs (see below). The region, which appeared to be the site of frequent provirus integrations in Gross A MuLV-induced thymomas, was designated *Gin-1*.

Molecular characterization of the *Gin-1* region. The unoccupied chromosomal region surrounding the sequences homologous to the SS8 probe was further characterized by restriction enzyme analysis of normal mouse cellular DNA. By using different restriction endonucleases alone or in combination, it was possible to derive a partial restriction map of the region (data not shown) suitable for subsequent screening of thymoma DNAs and for gross mapping of the inserted proviruses.

To analyze this region in more detail and to derive additional probes necessary for a finer mapping of the inserted proviruses, we screened a partially *Eco*RI-digested phage library of thymoma 9 DNA and a partially *Hae*III-digested phage library of C57BL/6 DNA with probe SS8. Two positive clones (λ L985C and λ L982C) were obtained from the first library, and a third clone (λ LH81C) was obtained from the second library. These three overlapping clones spanned a region of about 26 kbp of cellular DNA. A restriction analysis of the cloned DNAs was performed (data not shown). This analysis allowed the derivation of a restriction map of the *Gin-1* region (Fig. 3). Furthermore, several single-copy hybridization probes (Fig. 3, A to E and U to Z), spanning most of the cloned *Gin-1* region, were prepared by subcloning several fragments from the three lambda clones into pBR322 or SP64.

Detection of proviruses integrated with the *Gin-1* region of Gross A MuLV-induced thymoma DNAs. To determine whether *Gin-1* was a common region for provirus integration in Gross A MuLV-induced thymomas, we screened a total of 40 Gross A MuLV-induced thymoma DNAs digested with *Eco*RI, *Hin*dIII, or *Kpn*I and hybridized them with the SS8 probe. *Eco*RI, *Hin*dIII, and *Kpn*I allowed the screening, respectively, of 5.4-, 14-, and 30-kbp regions of *Gin-1* (Fig. 3). *Hin*dIII cleaved the Gross A MuLV genome once (56). *Kpn*I cleaved within the Gross A LTR (or its MCF recombinant) provirus. *Eco*RI did not cleave the Gross A MuLV genome (56), but did cleave the MCF MuLV genome once at

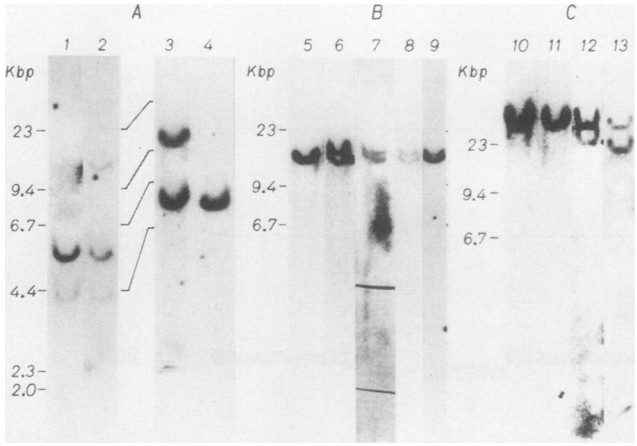

FIG. 4. Analysis of thymomas containing a novel DNA fragment homologous to probe SS8. DNAs (15 μg) from representative thymomas were digested with *Eco*RI (A), *Hin*dIII (B), or *Kpn*I (C), fractionated by electrophoresis on a 0.8% agarose gel, transferred to nitrocellulose membranes, and hybridized with a ^{32}P-labeled SS8 probe. DNAs from (A) thymomas 30, 9, 49, and 47 digested with *Eco*RI (lanes 1 to 4, respectively); (B) thymomas 34, 44, 50, 42, and 33 digested with *Hin*dIII (lanes 5 to 9, respectively); (C) thymomas 7, 8, 4, and 44 digested with *Kpn*I (lanes 10 to 13, respectively). Fragment size was estimated by using *Hin*dIII-digested λ DNAs as markers.

position 6.9 (Fig. 1). Of the 40 DNAs from the Gross A MuLV-induced tumors analyzed, 11 showed novel fragments in addition to the normal cellular fragment of the unoccupied remaining allele (Fig. 4, Table 1). These results suggested that *Gin-1* was a common region for provirus integration.

Structural organization of proviruses in the *Gin-1* region. If the novel DNA fragments detected in some thymoma DNAs with the SS8 probe were generated because of the insertion of a provirus in this region, the same fragments should be detected with virus-specific probes. To test this hypothesis, DNAs from thymomas 33 and 44 were digested with *Bam*HI and *Eco*RI, respectively, and were hybridized with the *Gin-1* probes B and E, respectively (Fig. 3). The novel 4.6-kbp *Bam*HI and 18-kbp *Eco*RI fragments were clearly observed in each tumor (Fig. 5, lanes 1 and 3). The same filters were washed, reexposed to monitor the absence of signals, and hybridized with a mixture of AKV-5 and AKV-6 viral probes. As expected, several virus-specific fragments were detected. One of these fragments comigrated exactly with the novel fragment previously detected with the *Gin-1* probes (Fig. 5, lanes 2 and 4), suggesting the presence of viral and *Gin-1* sequences on the same fragment. Because most of the tumor DNAs harbored numerous virus-specific fragments of a length similar to that of the novel *Gin-1* fragments, the results of this experiment with the other thymoma DNAs were not conclusive (data not shown).

Therefore, to determine whether the novel *Gin-1*-specific fragments were generated by the insertion of a provirus, to map the integration site of the provirus more precisely, and to determine the orientation of the integrated provirus relative to the *Gin-1* region, we performed a restriction analysis of the tumor DNAs by using a *Gin-1* probe closer to the integration site. A representative example of this analysis is presented in Fig. 6. DNA from thymoma 33 was digested with *Eco*RI, *Pst*I, or *Bam*HI and hybridized with the SS8 probe; no novel fragment could be detected with *Eco*RI or *Pst*I digestions (data not shown), but a novel 6.0-kbp *Bam*HI fragment was observed (Fig. 6, lane 2). Hybridization of *Eco*RI-digested thymoma 33 DNA with probe B did not reveal a novel fragment (data not shown). These results indicated that the provirus was integrated within the *Bam*HI fragment; more precisely it was located within the 300-base-pair *Pst*I-*Eco*RI fragment upstream of fragment B (probe B). DNA from this tumor was then digested with *Pst*I and hybridized with probe B. A 2.2-kbp novel fragment was detected in addition to the normal 1.9-kbp *Pst*I fragment (Fig. 6, lane 4), indicating the presence of a novel *Pst*I site within this region and confirming the insertion site of the provirus. The orientation of the provirus was determined with a double digestion (*Pst*I-*Kpn*I), which generated a 1.9-kbp novel fragment comigrating with the normal fragment (Fig. 6, lane 3). The difference in length between the novel 2.2-kbp *Pst*I fragment and the novel 1.9-kbp *Pst*I-*Kpn*I fragment corresponded to the distance separating these two

TABLE 1. Restriction enzyme analysis of the *Gin-1* region containing proviruses in 11 independent thymomas

Type of DNA	Type of provirus inserted[a]	Mouse strain	Fragment size (kbp) after digestion with probe[b]:										
			SS8 hybridized to:							B hybridized to:			E hybridized to
			K	B	B-K	H	H-K	E	E-K	E-K	P	P-K	E
Liver DNA		SIM.S	30	7.0	7.0	14	14	5.4	5.4	8.7	1.9	1.9	8.7
Tumors[c]													
1	MCF	SIM.S	20	8.6	5.6	23	14	N	ND	1.2	ND	ND	10
4	MCF	SIM.S	20	8.6	5.6	23	14	N	ND	1.2	1.3, 1.0	1.0, 1.0	10
9[d]	MCF	SIM.S	20, 15	8.9, 4.3	ND	11, 14	ND	4.1, 11	2.3, 5.5	ND	ND	ND	ND
30[e]	MCF	SIM.S	7.7	9.0	ND	8.7	ND	4.1	2.4	ND	ND	ND	ND
33	?	SIM.S	20	6.0	4.7	15	13	N	ND	N	2.2	1.9	ND
42	?	SIM.S	ND	ND	ND	16	ND	N	ND	ND	ND	ND	ND
44	ECO	NIH	20	7.5	6.2	16	ND	N	ND	1.8, 7.5	1.6, 0.7	1.6, 0.4	18
49	?	SIM.S	20	ND	ND	ND	ND	15	ND	ND	ND	ND	ND
50	MCF	SIM.S	20	7.7	6.4	16	ND	N	ND	2.0, 7.3	ND	ND	ND
54	MCF	SIM.S	20	6.6	5.3	16	ND	N	ND	0.95	1.55, 0.75	1.25, 0.75	10
70	MCF	SIM.S	20	6.7	5.4	16	14	N	ND	1.0	1.5, 0.8	1.5, 0.8	10

[a] The presence (MCF type) or the absence (ecotropic type) of an *Eco*RI site at position 6.9 was used as the criterion for this classification.
[b] Abbreviations: B, *Bam*HI; H, *Hin*dIII; K, *Kpn*I; P, *Pst*I; N, normal fragment only; ND, not done.
[c] In each tumor, the normal fragment seen in liver DNA was also detected.
[d] A second novel fragment which did not contain viral sequences was detected in this tumor.
[e] *Gin-1* region was rearranged by a provirus insertion and by another unknown event.

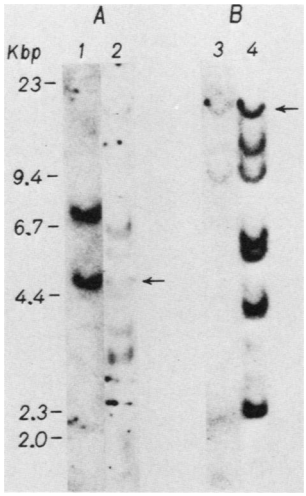

FIG. 5. Comigration of a novel fragment hybridizing with both *Gin-1* and p15E viral probes in thymomas 33 and 44. DNAs from thymomas 33 and 44 were digested with *Bam*HI and *Eco*RI, respectively, and were electrophoresed on a 0.8% agarose gel. DNA fragments were transferred to nitrocellulose membranes and hybridized with ^{32}P-labeled *Gin-1* probe E for thymoma 44 and with probe B for thymoma 33. The filters were then washed at 90°C for 1 h in 0.1× SSC-0.1% sodium dodecyl sulfate, reexposed to monitor the efficiency of the washing procedure, and rehybridized with ^{32}P-labeled AKV-5 and AKV-6 viral probes. (A) *Bam*HI-digested thymoma 33 DNA hybridized with *Gin-1* probe B (lane 1) or with AKV-5 and AKV-6 viral probes (lane 2). (B) *Eco*RI-digested thymoma 44 DNA hybridized with *Gin-1* probe E (lane 3) or with AKV-5 and AKV-6 viral probes (lane 4). The arrows indicate the fragment hybridizing with both probes.

sites within the Gross A LTR. We confirmed the orientation of the provirus with *Bam*HI and *Bam*HI-*Kpn*I digestions (Fig. 6, lanes 1 and 2), which generated novel fragments predicted by the insertion of a provirus. The results of this restriction analysis showed that the provirus was inserted 100 base pairs from the first *Pst*I site downstream of the SS8 sequences, in the orientation 5′ to 3′ (Fig. 6).

To map the provirus in tumor 44, DNA was digested with a combination of *Eco*RI and *Kpn*I and hybridized with probe B. *Kpn*I was chosen because it cleaved the provirus within the LTR and therefore allowed more precise mapping. Under these conditions, three fragments were detected: two *Eco*RI-*Kpn*I fragments (1.8 and 7.5 kbp) and one *Eco*RI fragment (8.7 kbp) (Fig. 6, lane 7). The 8.7-kbp *Eco*RI fragment corresponded to the fragment from the unoccupied and unrearranged normal allele, since it was the only fragment detected in normal DNA. This digestion indicated that a novel *Kpn*I site was close to the *Eco*RI site bordering probe B, and we therefore placed the site of insertion of the provirus quite precisely, depending on its orientation, at a maximal distance of 1.5 kbp from the *Eco*RI site. To determine the orientation of the provirus, the same tumor DNA was digested with *Pst*I (which cleaves within the LTR) and was hybridized with the same probe (B). Again, three *Pst*I fragments could be detected, i.e., two novel fragments of 1.6 and 0.7 kbp, in addition to the normal 1.9-kbp fragment (Fig. 6, lane 6). When a double digestion with *Pst*I-*Kpn*I was performed, the novel 1.6-kbp *Pst*I fragment was not cleaved with *Kpn*I, but the novel 0.7-kbp *Pst*I fragment, harboring sequences downstream of the proviral insertion site, was cleaved once to generate one detectable *Pst*I-*Kpn*I fragment of 0.4 kbp (Fig. 6, lane 5). These results indicated that provirus was integrated in tumor 44 at 300 base pairs from the *Pst*I site bordering probe B, in a 5′ to 3′ orientation (Fig. 6). Because of the length of the *Eco*RI-*Kpn*I novel fragment hybridizing with probe B (1.8 kbp) in tumor 44, an opposite orientation would not agree with the other results obtained and would place the integration site downstream of the *Pst*I site bordering probe B, i.e., beyond probe B detection.

An approach similar to that for tumor 44, with the same restriction endonucleases and the same hybridizing probes, was used to map the provirus in tumor 54 (Fig. 6, lanes 8–10). To further confirm the orientation of this provirus in tumor 54, an *Eco*RI digestion was performed, and the DNA fragments were hybridized with probe E. A novel 10.2-kbp *Eco*RI fragment was detected in this tumor in addition to the normal 8.7-kbp fragment (Fig. 6, lane 11). The difference in length between this novel 10.2-kbp *Eco*RI fragment and the novel 8.4-kbp *Eco*RI-*Kpn*I fragment corresponded to the distance separating the *Eco*RI within an MCF provirus and the *Kpn*I site within the LTR. Moreover, the integration of the provirus in an opposite orientation would have generated a 15-kbp *Eco*RI fragment. Therefore, in thymoma 54, the provirus was integrated at 450 base pairs from the *Eco*RI site bordering probe B, in the orientation shown in Fig. 6.

Fine mapping of each provirus integrated within *Gin-1* was performed in a similar way, and a summary of the results from most digestions is presented in Table 1. A map of *Gin-1* with the precise integration site of the provirus and its orientation for each positive thymoma detected is shown in Fig. 7. The proviruses were all integrated as a cluster within a 5-kbp region of *Gin-1*. Interestingly, except for the provirus in thymoma 42, which has not been oriented, the proviruses were all integrated in the same orientation relative to *Gin-1*. Most of the inserted proviruses (seven of eight which could be studied with certainty) had an MCF-type structure, as judged by the presence of an *Eco*RI site at position 6.9. Only one inserted provirus of the eight proviruses studied had the structure of the inoculated ecotropic Gross A MuLV (absence of the internal *Eco*RI site).

***Gin-1* maps on mouse chromosome 19.** To map the *Gin-1* single-copy sequences to a specific chromosome, we used a series of hamster-mouse somatic-cell hybrids which had segregated different mouse chromosomes. The cell hybrids were generated by fusion of Chinese hamster cells (E36) with peritoneal cells or spleen cells of BALB/c, A/J, and NFS/Akv-2 congenic mice. The characterization of these hybrids and their uses in the chromosomal mapping of other cellular genes have been described elsewhere (25–27). DNAs from these cell hybrids were cleaved with *Eco*RI and analyzed by the Southern blotting technique with the SS8 probe. Under the conditions of hybridization used, the probe did not hybridize to hamster cell DNA. A total of 25 hybrid cell DNAs were analyzed by this method. Figure 8 shows a representative example of the results. All hybrid DNAs analyzed were scored as positive or negative for the presence of the 5.4-kbp *Eco*RI fragment homologous to the SS8 probe. The mouse chromosomal content of these hybrids revealed that, except for one, clones positive for the presence of *Gin-1* sequences also carried mouse chromosome 19 and that all clones which did not harbor the 5.4-kbp *Eco*RI *Gin-1* fragment were also negative to chromosome 19 (Table 2). Therefore, these results indicated that the mouse *Gin-1* fragment maps to chromosome 19.

***Gin-1* is not homologous to known oncogenes.** To determine whether the *Gin-1* region contained sequences homologous

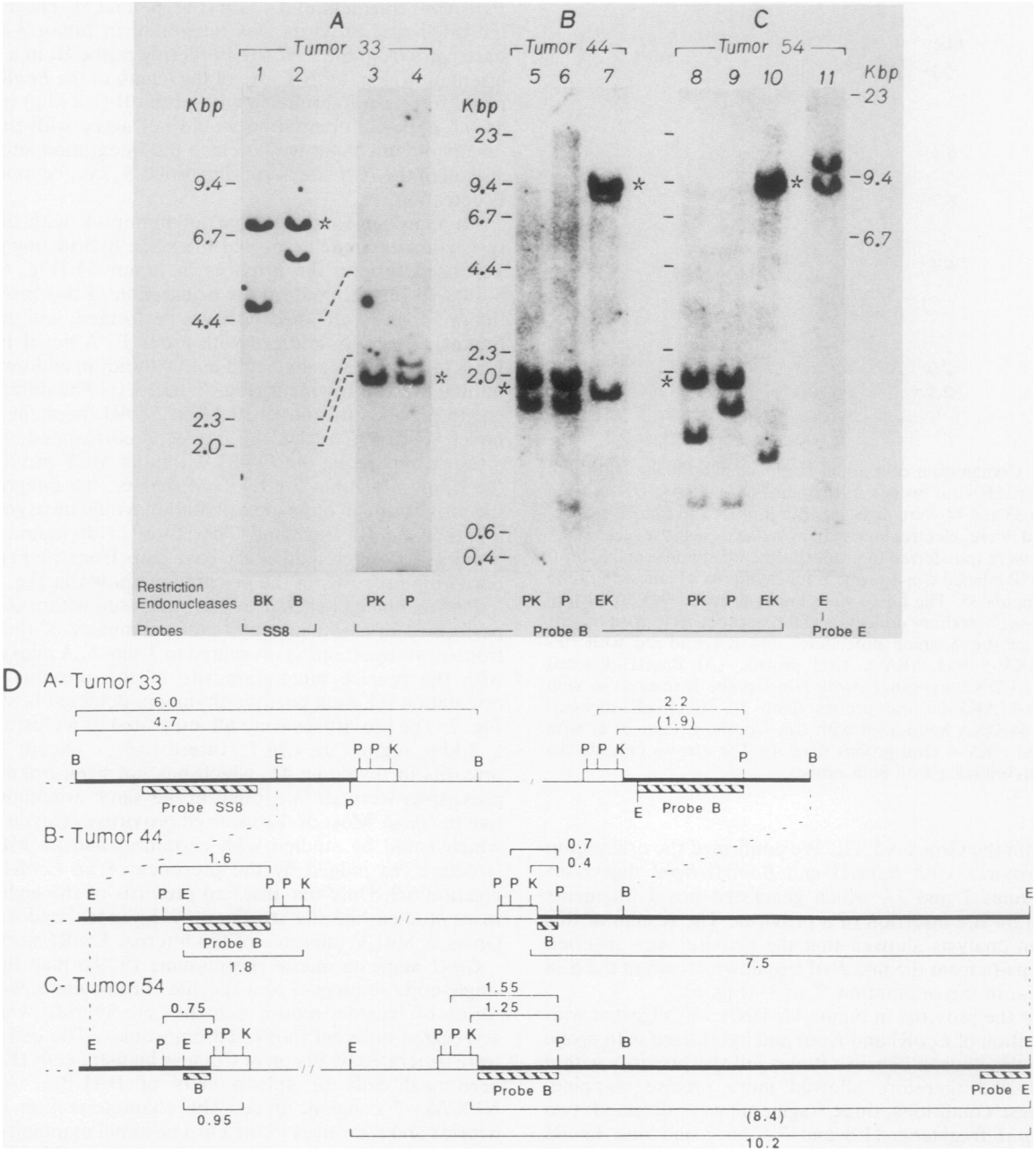

FIG. 6. Localization and orientation of three representative proviral insertions within the *Gin-1* region. DNAs (15 μg) from thymomas 33 (A), 44 (B), and 54 (C) were digested with restriction endonucleases, electrophoresed on 1.0% (lanes 1, 2, and 11) or 1.2% (lanes 3 to 10) agarose gels, transferred to nitrocellulose membranes, and hybridized with ^{32}P-labeled probe SS8 (lanes 1 and 2), probe B (lanes 3 to 10), or probe E (lane 11). Digestions for lanes: 1, *Bam*HI-*Kpn*I; 2, *Bam*HI; 4, 6, and 9, *Pst*I; 3, 5, and 8, *Pst*I-*Kpn*I; 7 and 10, *Eco*RI-*Kpn*I; 11, *Eco*RI. For each digestion, the fragment generated from the normal unoccupied allele and also found in normal DNA is indicated by an asterisk. At the bottom is the corresponding partial restriction map of the novel DNA fragments in each tumor. Symbols: ▭, LTR; ▨, probes; ——, viral sequences; ▬▬, cellular *Gin-1* sequences. Numbers in parentheses indicate fragments comigrating with the unoccupied normal fragment. Restriction endonucleases: B, *Bam*HI; E, *Eco*RI; K, *Kpn*I; P, *Pst*I.

to known oncogenes, we hybridized *Eco*RI-digested DNA from the two lambda clones, λ L985C and λ L982C, at high stringency with ^{32}P-labeled DNA fragments of v-*onc* or of cDNA from c-*onc* (1, 55). We found no hybridization of *Gin-1* sequences with sequences from *abl*, *erbA*, *erbB*, *ets*, *fms*, *fos*, *fps*, *mos*, *myb*, *myc*, p53, *ras*^{H}, *ras*^{K}, *ras*^{N}, *ros*, and *sis* (data not shown).

Specificity of provirus integration within *Gin-1*. The frequency of occupancy of *Pim-1* (8) or *myc* (36) by proviruses has been previously shown to be associated with, respectively, the early and late stages of leukemogenesis in MuLV-induced T-cell leukemias. To determine whether the frequency of *Gin-1* occupancy varied in T-cell tumors induced by different MuLV strains in different mouse strains, we screened 17 spontaneous AKR thymoma DNAs and 11 DNAs from SL3-3-induced thymomas of NFS mice with the

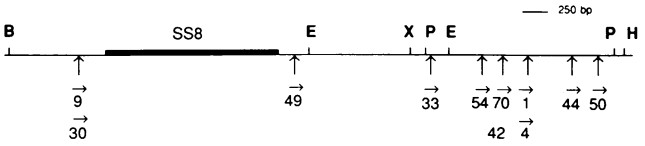

FIG. 7. Location and orientation of the proviruses integrated within the *Gin-1* region. An expanded view of a segment of the *Gin-1* region where all integrations detected occurred. The orientation of provirus in tumor 42 has not been determined. Symbols: ↑, site of provirus integration; →, orientation of provirus 5′ to 3′. Numbers are thymoma designations. Restriction endonucleases are abbreviated as defined in the legend to Fig. 3.

Gin-1 SS8 probe to detect rearrangements within the *Gin-1* region. In none of these tumor DNAs did we observe a novel *Kpn*I fragment with the SS8 probe (Table 3). In contrast, the *myc* locus was found rearranged in a low percentage of the tumors analyzed, including those induced by Gross A MuLV. The three Gross A tumors positive for *myc* rearrangement were negative for *Gin-1* occupancy. These results suggested that provirus integration within *Gin-1* was MuLV or mouse strain specific or both.

The frequency of provirus integration within *Gin-1* was compared with the time of appearance of the disease. We found no obvious correlation between the latent period of the disease and the frequency of *Gin-1* occupancy.

DISCUSSION

In an effort to understand the molecular mechanism by which nondefective Gross A MuLV induced T-cell leukemia, we tested the insertional mutagenesis model. This model holds that one of the genetic events leading to tumor formation is the activation of a cellular oncogene by the integration of a provirus in its vicinity. A prediction of this model is that at least one provirus in each tumor will be integrated within the same chromosomal region as in some other tumors and that such a common integration region will harbor an oncogene.

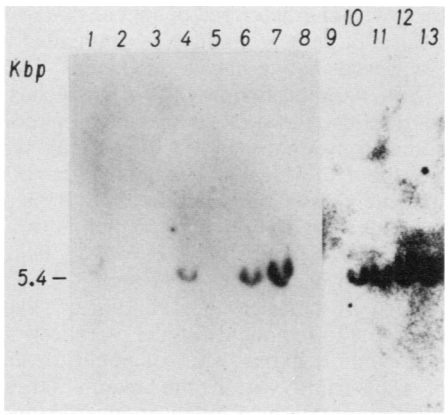

FIG. 8. Hybridization of the SS8 *Gin-1* probe with mouse, Chinese hamster, and hybrid cell DNAs. DNAs (5 μg) were digested with *Eco*RI, electrophoresed on a 1% agarose gel, transferred to nitrocellulose membranes, and hybridized with a ^{32}P-labeled SS8 probe. DNAs were from NIH/Swiss mouse liver (lane 1), E36 Chinese hamster cells (lane 2), and hybrids HM32 (lane 3), HM34 (lane 4), HM36 (lane 5), HM38 (lane 6), HM46 (lane 7), HM49 (lane 8), HM59 (lane 9), HM61 (lane 10), HM62 (lane 11), HM63 (lane 12), and HM64 (lane 13).

TABLE 2. Correlation of mouse chromosomes and *Gin-1* in 25 hybrid clones

Mouse chromosome no.	No. of hybrid clones with *Gin-1*/ chromosome retention				% Discordant
	+/+	−/−	+/−	−/+	
1	8	5	4	5	41
2	7	6	5	4	41
3	3	5	2	3	39
4	7	7	4	3	33
5	2	9	11	1	52
6	8	6	5	4	39
7	11	3	2	7	39
8	6	7	6	3	41
9	6	8	6	2	36
10	2	9	11	1	52
11	0	8	8	0	50
12	3	1	2	7	69
13	3	6	2	2	31
14	4	8	9	2	48
15	5	0	0	8	62
16	4	4	3	7	47
17	6	3	2	5	44
18	3	6	2	3	36
19	12	9	0	1	5
X	8	6	3	4	33

To test this model experimentally, we attempted to clone all the proviruses present in a single Gross A MuLV-induced thymoma, hoping to identify all the genetic events required for the induction of this retrovirus-induced tumor. We succeeded in cloning five of the six proviruses integrated in thymoma 9 DNA, and we found that one of these proviruses was inserted within a chromosomal region which happens to be occupied by proviruses in a significant percentage of the other Gross A MuLV-induced thymomas tested. This common region for Gross A MuLV provirus integration was designated *Gin-1*. It was found occupied by provirus in about 28% of Gross A MuLV-induced thymomas of SIM.S mice. Considering that provirus integration seemed to occur at random in the mouse genome, the integration of proviruses within a small region of the genome, such as *Gin-1*, in more than one-fourth of the tumors, represented a very significant clustering and suggested a strong association of this genetic event with tumor formation. However, the *Gin-1* region was not occupied by provirus in all thymomas, suggesting that another genetic event(s) important for tumor development and not involving *Gin-1* was occurring in the *Gin-1*-negative tumors. Some of these events could represent integration of a provirus in other well-defined regions already shown to be specific integration sites for proviruses or in other yet unidentified loci. Indeed, in three of the tumor DNAs

TABLE 3. Incidence of rearrangements of *Gin-1* and *myc* regions in retrovirus-induced mouse T-cell lymphomas

Type of thymomas analyzed	Mouse strain	No. of rearrangements			
		Gin-1[a]	Frequency (%)	*myc*[b]	Frequency (%)
Gross A induced	SIM.S	10/37	27	3/34	9
	NIH/Swiss	1/3	33		
SL3-3-induced[c]	NFS	0/11	0	1/11	9
Spontaneous	AKR	0/17	0	5/15	33

[a] *Gin-1* was screened with SS8 probe.
[b] *Kpn*I was used for screening of c-*myc*.
[c] DNAs kindly provided by Herbert C. Morse III.

screened, we documented integration within the *myc* locus. In fact, none of the common regions for provirus integration described to date have been found to be the target site for provirus integration in a very high proportion of the MuLV-induced tumors. On the contrary, most regions were found occupied by proviruses in a low percentage of the tumors, and only *Pim-1* was found occupied in more than 50% of some MuLV-induced tumors tested (8). Most likely, several possible factors could explain the relatively low frequency of provirus integration in each of the specific regions identified to date. One factor is probably the biology of the system itself. Interestingly, by using a well-defined virus-host system, O'Donnell et al. (36) were indeed able to show that the frequency of MuLV provirus integration in the vicinity of the mouse c-*myc* is dependent on the stage of leukemogenesis. Another factor might be the presence in the genome of several functionally similar genes which could be activated independently by a molecular event such as provirus integration to provide the cell with a growth advantage. Already, 16 specific chromosomal regions (five oncogenes [*myc*, *myb*, *erbB*, *tck*, and *mos*], two genes coding for growth factors [IL-2 and IL-3], and nine other less characterized regions [*int-1*, *int-2*, *int-4l*, *Mlvi-1*, *Mlvi-2*, *Mlvi-3*, *Mis-1/pvt-1*, *Pim-1*, and *Fis-1*]) have been shown to represent a common integration site for provirus in retrovirus-induced tumors, and possibly several other regions remain to be identified.

The frequency of provirus integration within *Gin-1* appears to be dependent on the virus strain inoculated or the mouse strain used or both. Indeed, we could not detect occupancy of the *Gin-1* region in DNAs from other thymomas induced in different mouse strains by other MuLV strains (Table 3). The same kind of specificity has been observed for *Pim-1* (8) and *Fis-1* (47) in MuLV-induced mouse hematopoietic tumors and for *Mis-1/pvt-1* in Moloney MuLV-induced rat thymomas (L. Villeneuve and P. Jolicoeur, unpublished observations). But the nature of this specificity remains unclear.

Each mapped provirus found within *Gin-1* was integrated in the same 5′ to 3′ orientation, and all integrations occurred within 5 kbp of each other. Such integrated proviruses falling into a cluster in the same orientation had been observed previously near the oncogenes *myc*, *myb*, and *erbB*. In virus-induced bird or mouse tumors, the proviruses were most frequently found integrated upstream of avian c-*myc* (16, 33, 42) or c-*erbB* (15, 40) and of murine c-*myb* (46), in the same orientation, with the LTR as the promoter. However, in mouse T-cell lymphomas, proviruses were most frequently found integrated in a cluster upstream of the first exon of c-*myc* and in an opposite transcriptional orientation (7, 31, 43). Clustered insertion sites have also been observed within the other common regions for provirus integration, i.e., *int-1* (34, 35), *int-2* (13, 38), *Pim-1* (8), and *Mis-1/pvt-1* (18, 29, 57). Among the regions in which a transcription unit has been identified, namely, *int-1* (34, 35), *int-2* (12, 38), and *Pim-1* (44), the proviruses were found integrated within two domains, either upstream of the transcription unit, generally in an opposite orientation, or downstream of the transcription unit in the same orientation. We have not yet observed two domains of integration within the 30 kbp of *Gin-1* region that we screened. But, if a similar molecular mechanism operates in *Gin-1* as in the other regions, then by analogy with previous findings, the clustered integration sites identified may be downstream or upstream of a transcription unit. The fact that the proviruses had integrated as a cluster, and all in the same orientation, indeed suggested a specific molecular requirement for this genetic event to be significant for T-cell transformation, assuming that the *Gin-1* region plays some role in leukemogenesis.

Most of the proviruses found within *Gin-1* had a recombinant structure, as judged by the presence of an *Eco*RI site in the *env* region at position 6.9. Although we can rely only on this single criterion to classify these recombinant proviruses, they most likely represent the genome of MCF-type MuLVs, already found to be present in several other MuLV-induced lymphomas (13) and more specifically in thymomas induced by SL3-3 MuLV, a virus related to Gross A MuLV (50). In most of the thymoma DNAs analyzed, these recombinant genomes appeared to be more numerous than proviruses from the inoculated parental ecotropic MuLV. In thymoma 9, from which we cloned five of the six integrated proviruses, three had a recombinant structure with an *Eco*RI site in *env*. All three proviruses had conserved the LTR of the parental inoculated ecotropic Gross A MuLV, which typically contains two *Pst*I sites within its U3 region. Since the recombinant MuLV proviruses were found to be more numerous in each thymoma DNA than in the parental ecotropic Gross A MuLV genomes, it was not unexpected that they constituted the majority of proviruses found integrated within *Gin-1*. However, several other biological or molecular factors could specifically favor the preferential choice of a recombinant provirus to integrate within *Gin-1*. It remains to be determined whether this event reflects the higher copy number of these proviruses or a more specific requirement.

By using mouse-hamster cell hybrids, we mapped the unique copy sequence of the *Gin-1* region on mouse chromosome 19. Because of this chromosomal location, *Gin-1* is distinct from *int-1* and *int-2*, which map on mouse chromosomes 15 (34, 39) and 7 (39), respectively. *Gin-1* also maps on a different chromosome than *Pim-1* (chromosome 17) (22), *Mis-1/pvt-1* (chromosome 15) (18, 24), *Mlvi-1*, *Mlvi-2* (chromosome 15) (28, 53), and *Fis-1* (chromosome 7) (47). The restriction map of the *Gin-1* region is distinct from those of *Mlvi-3* (51, 52) and *int-4l* (17). Moreover, we found no homology of *Gin-1* with 16 oncogenes tested, and no oncogene has yet been reported to map on mouse chromosome 19. Therefore, *Gin-1* appears to be a new common region for provirus integration.

Among such regions previously described, three regions harbor already well characterized oncogenes (*myc*, *myb*, and *erbB*), and three other regions harbor sequences which are thought to represent new putative oncogenes (*Pim-1*, *int-1*, and *int-2*). Still another region (*Mis-1/pvt-1*) has recently been shown to be also the site of a specific breakpoint during a chromosomal translocation [6; 15] in B-cell lymphomas (18, 57). So the *Gin-1* region might also contain a new cellular oncogene whose transcription might be activated by the specific integration of a provirus, which is true for *myc*, *myb*, *int-1*, *int-2*, *erbB*, and *Pim-1*. However, using various *Gin-1* probes, we were unable to detect RNA transcripts from this region in a variety of cell types. This negative result could be due to technical defects (very low abundance of mRNA, very short exons, etc.) or could mean the total absence of transcripts within the region screened, the provirus possibly acting at a much greater distance. Alternatively, the integration of a provirus within *Gin-1* might disrupt specific sequences whose integrity is required for regulated cell growth. The provirus could be inactivating the transcription of a gene not expressed in the normal or malignant cell types we tested but expressed only in some normal subpopulation of T cells which are the target for Gross A MuLV transformation. Since only one of the *Gin-1* alleles is in general occupied by a provirus, this model also

assumes that the expression of the normal *Gin-1* allele would not be sufficient to prevent transformation. Whatever the underlying molecular mechanism, the integration of a provirus within *Gin-1* is likely to be one of the important events leading to T-cell transformation after Gross A MuLV inoculation, and the *Gin-1* region may harbor sequences which are involved in tumor development.

ACKNOWLEDGMENTS

This work was supported by grants from the Medical Research Council of Canada to P.J. and E.R. and from the National Cancer Institute of Canada to P.J. R.V. is the recipient of a studentship from the Fonds de la Recherche en Santé du Québec, and Y.M. is the recipient of a studentship from the Cancer Research Society, Inc. (Montreal).

We thank Luc DesGroseillers for providing some tumor DNAs. We thank Benoît Laganière for his excellent technical assistance.

LITERATURE CITED

1. **Bishop, J. M.** 1983. Cellular oncogenes and retroviruses. Annu. Rev. Biochem. **52**:350–354.
2. **Buchhagen, D. L., F. S. Pedersen, R. L. Crowther, and W. A. Haseltine.** 1980. Most sequence differences between the genomes of the AKV virus and a leukemogenic Gross A virus passage in vitro are located near the 3′ terminus. Proc. Natl. Acad. Sci. USA **77**:4359–4363.
3. **Canaani, E., O. Dreazen, A. Klar, G. Rechavi, D. Ram, J. B. Cohen, and D. Givol.** 1983. Activation of the c-*mos* oncogene in a mouse plasmacytoma by insertion of an endogenous intracisternal A-particle genome. Proc. Natl. Acad. Sci. USA **80**:7118–7122.
4. **Chatis, P. A., C. A. Holland, J. W. Hartley, W. P. Rowe, and N. Hopkins.** 1983. Role of the 3′ end of the genome in determining disease specificity of Friend and Moloney murine leukemia viruses. Proc. Natl. Acad. Sci. USA **80**:4408–4411.
5. **Chattopadhyay, S. K., M. R. Lander, E. Rands, and D. R. Lowy.** 1980. Structure of endogenous murine leukemia virus DNA in mouse genomes. Proc. Natl. Acad. Sci. USA **77**:5774–5778.
6. **Chen, S. J., N. J. Holbrook, K. F. Mitchell, C. A. Vallone, J. S. Greengard, G. R. Crabtree, and Y. Lin.** 1985. A viral long terminal repeat in the interleukin 2 gene of a cell line that constitutively produces interleukin 2. Proc. Natl. Acad. Sci. USA **82**:7284–7288.
7. **Corcoran, L. M., J. M. Adams, A. R. Dunn, and S. Cory.** 1984. Murine T lymphomas in which the cellular myc oncogene has been activated by retroviral insertion. Cell **37**:113–122.
8. **Cuypers, H. T., G. Selten, W. Quint, M. Zijilstra, E. R. Maandag, W. Boelens, P. van Wezenbeek, C. Melief, and A. Berns.** 1984. Murine leukemia virus-induced T-cell lymphomagenesis: integration of proviruses in a distinct chromosomal region. Cell **37**:141–150.
9. **DesGroseillers, L., and P. Jolicoeur.** 1984. The tandem direct repeats within the long terminal repeat of murine leukemia viruses are the primary determinant of their leukemogenic potential. J. Virol. **52**:945–952.
10. **DesGroseillers, L., and P. Jolicoeur.** 1984. Mapping the viral sequences conferring leukemogenicity and disease specificity in Moloney and amphotropic murine leukemia viruses. J. Virol. **52**:448–456.
11. **DesGroseillers, L., R. Villemur, and P. Jolicoeur.** 1983. The high leukemogenic potential of Gross passage A murine leukemia virus maps in the region of the genome corresponding to the long terminal repeat and to the 3′ end of *env*. J. Virol. **47**:24–32.
12. **Dickson, C., R. Smith, S. Brookes, and G. Peters.** 1984. Tumourigenesis by mouse mammary tumour virus: proviral activation of a cellular gene in the common integration region int-2. Cell **37**:529–536.
13. **Famulari, N. G.** 1983. Murine leukemia viruses with recombinant *env* genes: a discussion of their role in leukemogenesis. Curr. Top. Microbiol. Immunol. **103**:75–108.
14. **Feinberg, A. P., and B. Vogelstein.** 1983. A technique for radiolabeling DNA restriction endonuclease fragments to high specific activity. Anal. Biochem. **132**:6–13.
15. **Fung, Y. K., W. G. Lewis, L. B. Crittenden, and H. J. Kung.** 1983. Activation of the cellular oncogene c-*erbB* by LTR insertion: molecular basis for induction of erythroblastosis by avian leukosis virus. Cell **33**:357–358.
16. **Fung, Y.-K. T., L. B. Crittenden, and H.-J. Kung.** 1982. Orientation and position of avian leukosis virus DNA relative to the cellular oncogene c-*myc* in B-lymphoma tumors of highly susceptible $15I_5 \times 7_2$ chickens. J. Virol. **44**:742–746.
17. **Garcia, M., R. Wellinger, A. Vessaz, and H. Diggelman.** 1986. A new site of integration for mouse mammary tumor virus proviral DNA common to BALB/cf (C3H) mammary and kidney adenocarcinomas. EMBO J. **5**:127–134.
18. **Graham, M., J. M. Adams, and S. Cory.** 1985. Murine T lymphomas with retroviral inserts in the chromosomal 15 locus for plasmacytoma variant translocations. Nature (London) **314**:740–743.
19. **Gross, L.** 1970. Oncogenic viruses. Pergamon Press, Inc., Elmsford, N.Y.
20. **Hayward, W. S., B. G. Neel, and S. M. Astrin.** 1981. Activation of a cellular *onc* gene by promoter insertion in ALV-induced lymphoid leukosis. Nature (London) **290**:475–480.
21. **Herr, W., D. Schwartz, and W. Gilbert.** 1983. Isolation and mapping of cDNA hybridization probes specific for ecotropic and nonecotropic murine leukemia proviruses. Virology **125**:139–154.
22. **Hilkens, J., H. T. Cuypers, G. Selten, V. Kroezen, J. Hilgers, and A. Berns.** 1985. Genetic mapping of Pim-1 putative oncogene to mouse chromosome 17. Somatic Cell Mol. Genet. **12**:81–88.
23. **Holland, C. A., J. W. Hartley, W. P. Rowe, and N. Hopkins.** 1985. At least four viral genes contribute to the leukemogenicity of murine retrovirus MCF 247 in AKR mice. J. Virol. **53**:158–165.
24. **Jolicoeur, P., L. Villeneuve, E. Rassart, and C. Kozak.** 1985. Mouse chromosomal mapping of a murine leukemia virus integration region (*Mis-1*) first identified in rat thymic leukemia. J. Virol. **56**:1045–1048.
25. **Kozak, C. A., E. Nichols, and F. H. Ruddle.** 1975. Gene linkage analysis in the mouse by somatic cell hybridization assignment of adenosine phosphoribosyl transferase to chromosome 8 and α-galactosidase to the X chromosome. Somatic Cell Mol. Genet. **1**:371–382.
26. **Kozak, C. A, and W. P. Rowe.** 1979. Genetic mapping of ecotropic murine leukemia-virus inducing locus of BALB/c mice to chromosome 5. Science **204**:69–71.
27. **Kozak, C. A., and W. P. Rowe.** 1980. Genetic mapping of the ecotropic virus inducing locus (Akv-2) of the AKR mouse. J. Exp. Med. **150**:1419–1423.
28. **Kozak, C. A., P. G. Strauss, and P. N. Tsichlis.** 1985. Genetic mapping of a cellular DNA region involved in induction of thymic lymphomas (*Mlvi-1*) to mouse chromosome 15. Mol. Cell. Biol. **5**:894–897.
29. **Lemay, G., and P. Jolicoeur.** 1984. Rearrangement of a DNA sequence homologous to a cell-virus junction fragment in several Moloney murine leukemia virus-induced rat thymomas. Proc. Natl. Acad. Sci. USA **81**:38–42.
30. **Lenz, J., D. Celander, R. L. Crowther, R. Patar, D. W. Perkins, and W. A. Haseltine.** 1984. Determination of the leukemogenicity of a murine retrovirus by sequences within the long terminal repeat. Nature (London) **308**:467–470.
31. **Li, Y., C. Holland, J. Hartley, and N. Hopkins.** 1984. Viral integration near c-*myc* in 10%–20% of MCF 247-induced AKR lymphomas. Proc. Natl. Acad. Sci. USA **81**:6808–6811.
32. **Maniatis, T., E. F. Fritsch, and J. Sambrook.** 1982. Molecular cloning: a laboratory manual. Cold Spring Harbor Laboratory, Cold Spring Harbor, N.Y.
33. **Neel, B. G., W. S. Hayward, H. L. Robinson, J. Fang, and S. M. Astrin.** 1981. Avian leukosis virus-induced tumors have common proviral integration sites and synthesize discrete new

RNAs: oncogenesis by promoter insertion. Cell 23:323–334.
34. **Nusse, R., A. van Ooyen, D. Cox, Y. K. Fung, and H. Varmus.** 1984. Mode of proviral activation of a putative mammary oncogene (int-1) on mouse chromosome 15. Nature (London) 307:131–136.
35. **Nusse, R., and H. Varmus.** 1982. Many tumours induced by the mouse mammary tumour virus contain a provirus integrated in the same region of the host genome. Cell 31:99–109.
36. **O'Donnell, P. V., E. Fleissner, H. Lonial, C. F. Koehne, and A. Reicin.** 1985. Early clonality and high-frequency proviral integration into the c-*myc* locus in AKR leukemias. J. Virol. 55:500–503.
37. **Payne, G. S., J. M. Bishop, and H. E. Varmus.** 1982. Multiple arrangements of viral DNA and an activated host oncogene in bursal lymphomas. Nature (London) 295:209–214.
38. **Peters, G., S. Brookes, R. Smith, and C. Dickson.** 1983. Tumourigenesis by mouse mammary tumour virus: evidence for a common region for provirus integration in mammary tumours. Cell 33:369–377.
39. **Peters, G., C. Kozak, and C. Dickson.** 1984. Mouse mammary tumor virus integration regions *int-1* and *int-2* map on different mouse chromosomes. Mol. Cell. Biol. 4:375–378.
40. **Raines, M. A., W. G. Lewis, L. B. Crittenden, and H. J. Kung.** 1985. C-erbB activation in avian leukosis virus-induced erythroblastosis: clustered integration sites and the arrangement of provirus in the c-*erbB* alleles. Proc. Natl. Acad. Sci. USA 82:2287–2291.
41. **Rigby, P. W. J., M. Dieckmann, C. Rhodes, and P. Berg.** 1977. Labeling deoxyribonucleic acid to high specific activity in vitro by nick translation with DNA polymerase I. J. Mol. Biol. 113:237–257.
42. **Robinson, H. L., and G. C. Gagnon.** 1986. Patterns of proviral integration and deletion in avian leukosis virus-induced lymphomas. J. Virol. 57:28–36.
43. **Selten, G., H. Cuypers, M. Zijilstra, C. Melief, and A. Berns.** 1984. Involvement of c-*myc* in MuLV-induced T cell lymphomas in mice: frequency and mechanisms of activation. EMBO J. 3:3215–3222.
44. **Selten, G., H. T. Cuypers, and A. Berns.** 1985. Proviral activation of the putative oncogene Pim-1 in MuLV-induced T-cell lymphomas. EMBO J. 4:1793–1798.
45. **Shen-Ong, G. L. C., H. C. Morse III, M. Potter, and J. F. Mushinski.** 1986. Two modes of c-*myb* activation in virus-induced mouse myeloid tumors. Mol. Cell. Biol. 6:380–382.
46. **Shen-Ong, G. L. C., M. Potter, J. F. Mushinski, S. Lavu, and E. P. Reddy.** 1984. Activation of the c-*myb* locus by viral insertional mutagenesis in plasmacytoid lymphosarcoma. Science 226:1077–1080.
47. **Silver, J., and C. Kozak.** 1986. Common proviral integration region on mouse chromosome 7 in lymphomas and myelogenous leukemias induced by Friend murine leukemia virus. J. Virol. 57:526–533.
48. **Southern, E. M.** 1975. Detection of specific sequences among DNA fragments separated by gel electrophoresis. J. Mol. Biol. 38:503–517.
49. **Steffen, D.** 1984. Proviruses are adjacent to c-*myc* in some murine leukemia virus-induced lymphomas. Proc. Natl. Acad. Sci. USA 81:2097–2101.
50. **Thomas, C. Y.** 1986. AKR ecotropic murine leukemia virus SL3-3 forms envelope gene recombinants in vivo. J. Virol. 59:23–30.
51. **Tsichlis, P. N., L. Hu, and P. Straus.** 1983. Two common regions for proviral DNA integration in MoMuLV-induced rat thymic lymphomas. Implications for oncogenesis. ICN-UCLA Symp. Mol. Cell. Biol. 9:399–415.
52. **Tsichlis, P. N., P. Straus, and L. Hu.** 1983. A common region for proviral DNA integration in MoMuLV-induced rat thymic lymphomas. Nature (London) 302:445–449.
53. **Tsichlis, P. N., P. G. Strauss, and C. A. Kozak.** 1984. Cellular DNA region involved in induction of thymic lymphomas (*Mlvi-2*) maps to mouse chromosome 15. Mol. Cell. Biol. 4:997–1000.
54. **Tsichlis, P. N., P. G. Strauss, and M. A. Lohse.** 1985. Concerted DNA rearrangements in Moloney murine leukemia virus-induced thymomas: a potential synergistic relationship in oncogenesis. J. Virol. 56:258–267.
55. **Varmus, H.** 1984. The molecular genetics of cellular oncogenes. Annu. Rev. Genet. 18:553–612.
56. **Villemur, R., E. Rassart, L. DesGroseillers, and P. Jolicoeur.** 1983. Molecular cloning of viral DNA from leukemogenic Gross passage A murine leukemia virus and nucleotide sequence of its long terminal repeat. J. Virol. 45:539–546.
57. **Villeneuve, L., E. Rassart, P. Jolicoeur, M. Graham, and J. M. Adams.** 1986. Proviral integration site *Mis-1* in rat thymomas corresponds to the *pvt-1* translocation breakpoint in murine plasmacytomas. Mol. Cell. Biol. 6:1834–1837.
58. **Voronova, A. F., and B. M. Sefton.** 1986. Expression of a new tyrosine protein kinase is stimulated by retrovirus promoter insertion. Nature (London) 219:682–685.
59. **Ymer, S., W. Q. J. Tucker, C. J. Sanderson, A. J. Hapel, H. D. Campbell, and I. G. Young.** 1985. Constitutive synthesis of interleukin-3 by leukemia cell line WEH1-3B is due to retroviral insertion near the gene. Nature (London) 317:255–258.